JOURNAL OF MATERIALS SCIENCE **36** (2001) 4079–4088

Copper nucleation and growth during the corrosion of aluminum alloy 2524 in sodium chloride solutions

R. L. CERVANTES, L. E. MURR, R. M. ARROWOOD
Department of Metallurgical and Materials Engineering, The University of Texas at El Paso, El Paso, TX 79968-0520, USA

Copper clusters, as nodules and micro dendritic masses, were observed to nucleate and grow on Al 2524 surfaces after corrosion immersion experiments for up to 5 days in 0.6 M NaCl solutions; with pH values ranging from 3 to 11. Cu clusters observed by SEM on the corroded surfaces and confirmed by EDX analysis were extracted or stripped from their original sites and examined in detail utilizing TEM and EDX spectrometry. These observations confirm a mechanism contributing to pitting corrosion in copper-rich aluminum alloys involving the plating or cementation of Cu^{2+} from solution as an electrochemical displacement reaction, resulting in nucleation and growth of Cu clusters on the aluminum alloy surface, and causing additional aluminum dissolution and pitting around the Cu deposits.

1. Introduction

Obispo *et al*. [1] have recently observed clusters of copper nucleating and growing on the surface of 2024 aluminum alloy following free corrosion immersion experiments in 0.6 M NaCl solutions; over a pH range from 3 to 11. These observations were made by scanning electron microscopy (SEM) analysis of immersion coupons; with corresponding energy-dispersive X-ray spectrometer (EDX) analysis. In addition, a novel lift-off technique was employed to extract these copper clusters from the surface for more detailed observations and analysis in the transmission electron microscope (TEM). These copper deposits consisted of very fine microdendritic clusters in neutral to basic NaCl solutions (∼pH 6 to 11) while acidic NaCl solutions (pH 3) produced more nodular or botryoidal Cu clusters. These observations were consistent with electrochemical displacement reactions where copper in Cl^- solutions deposits (nucleates) onto the more electropositive Al or Al-alloy surface:

$$3Cu^{2+} + 2Al = 2Al^{3+} + 3Cu \text{ (clusters)} \quad (1)$$

As a result of this reaction, copper clusters nucleate and grow on the corroding surface. The low-overpotential cathodic behavior of the metalic copper promotes additional pitting corrosion, with additional release of Al^{3+} and some Cu^{2+}. The Cl^- ions help to keep the Al surface exposed where

$$Al \rightarrow Al^{3+} + 3\bar{e} \rightarrow \text{ (anodic)} \quad (2)$$

$$2H^+ + 2\bar{e} \rightarrow H_2 \text{ (cathodic)} \quad (3)$$

and

$$Al + 3OH^- \rightarrow Al(OH)_3 + 3\bar{e} \quad (4)$$

Under various conditions of pH and temperature, reaction (4) can be more complex and result in AlO(OH) or other oxy-hydroxides as well as $Al(OH)_3$ contributing to the corrosion products [2].

Chen *et al*. [3] have also observed Al-Cu-Mn-Fe-containing precipitate particles to act cathodically during aluminum alloy 2024 corrosion in slightly acidic NaCl solutions, and Cu was observed to plate on them (the exposed particles). However, copper clusters, similar to those observed by Obispo *et al*. [1], were also distributed at other, random surface sites [3], and the Cu deposit morphology tended to match those for corresponding pH ranges noted in the work by Obispo *et al*. [1].

The present investigation sought to confirm the deposition or nucleation of Cu and the growth of Cu clusters on aluminum alloy 2524 which has been considered as a replacement for commercial Al 2024 alloy, but which maintains essentially the same level of alloyed Cu (≥4 weight percent). Aluminum alloy 2524 sheet samples having the following composition (by weight percent) were sectioned into test coupons measuring 1.9 cm on a side: 4.5% Cu, 1.5% Mg, 0.64% Mn, 0.2% Fe, 0.19% Zn, 0.11% Si, 0.03% Ti, 0.02% Ni; balance Al. The samlpes were in the as-received (T3) temper.

These coupons were polished to a uniform surface finish with SiC papers and a fine surface polish achieved by using a colloidal SiO_2 (∼0.02 μm particle size). Representative coupons were then immersed in 3.5%

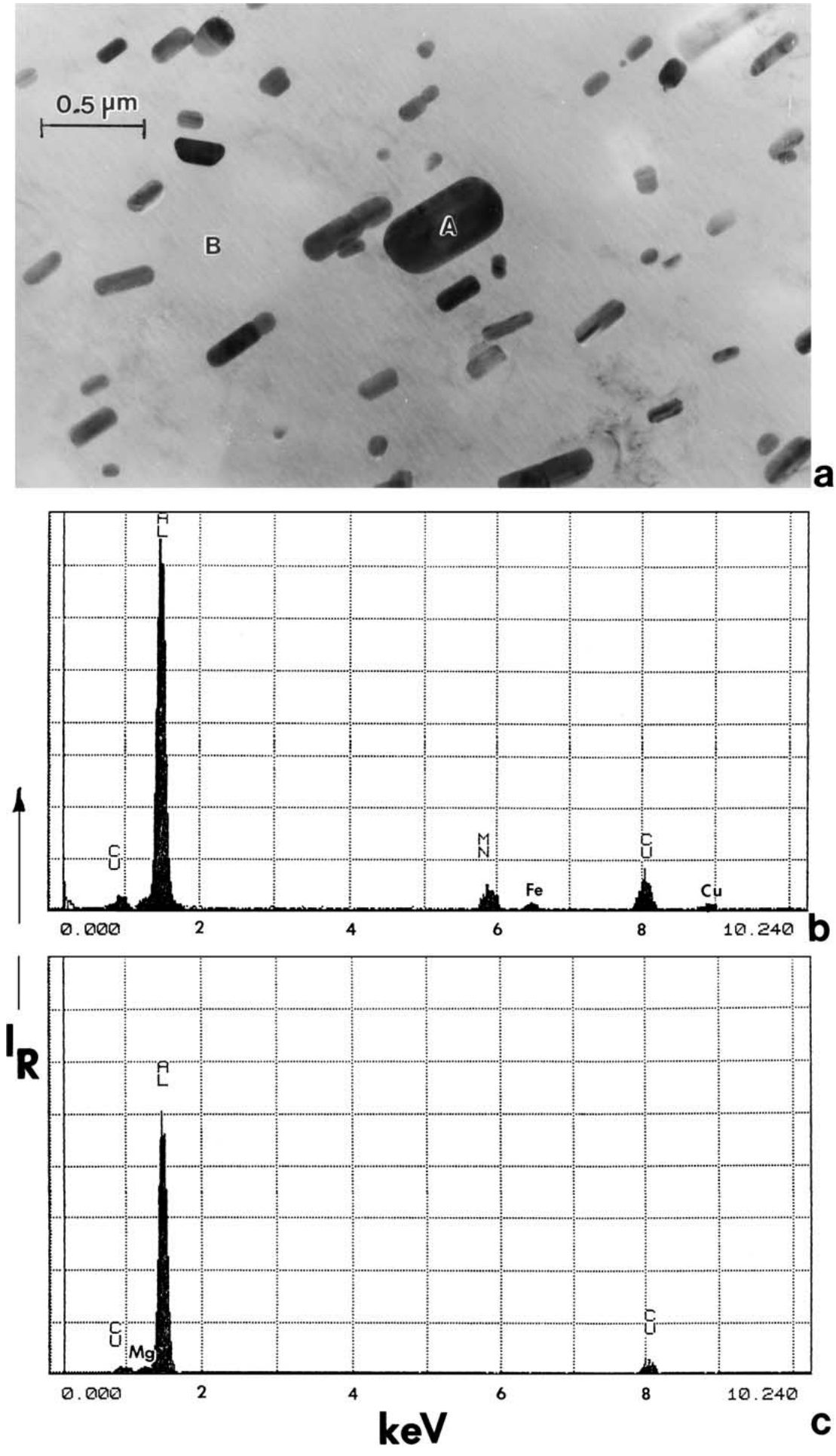

Figure 1 Typical example of precipitation/second-phase particles in aluminum alloy 2524. (a) Bright-field TEM image. (b) EDX spectrum for particle marked A in (a). (c) EDX reference spectrum for alloy matrix region marked B in (a).

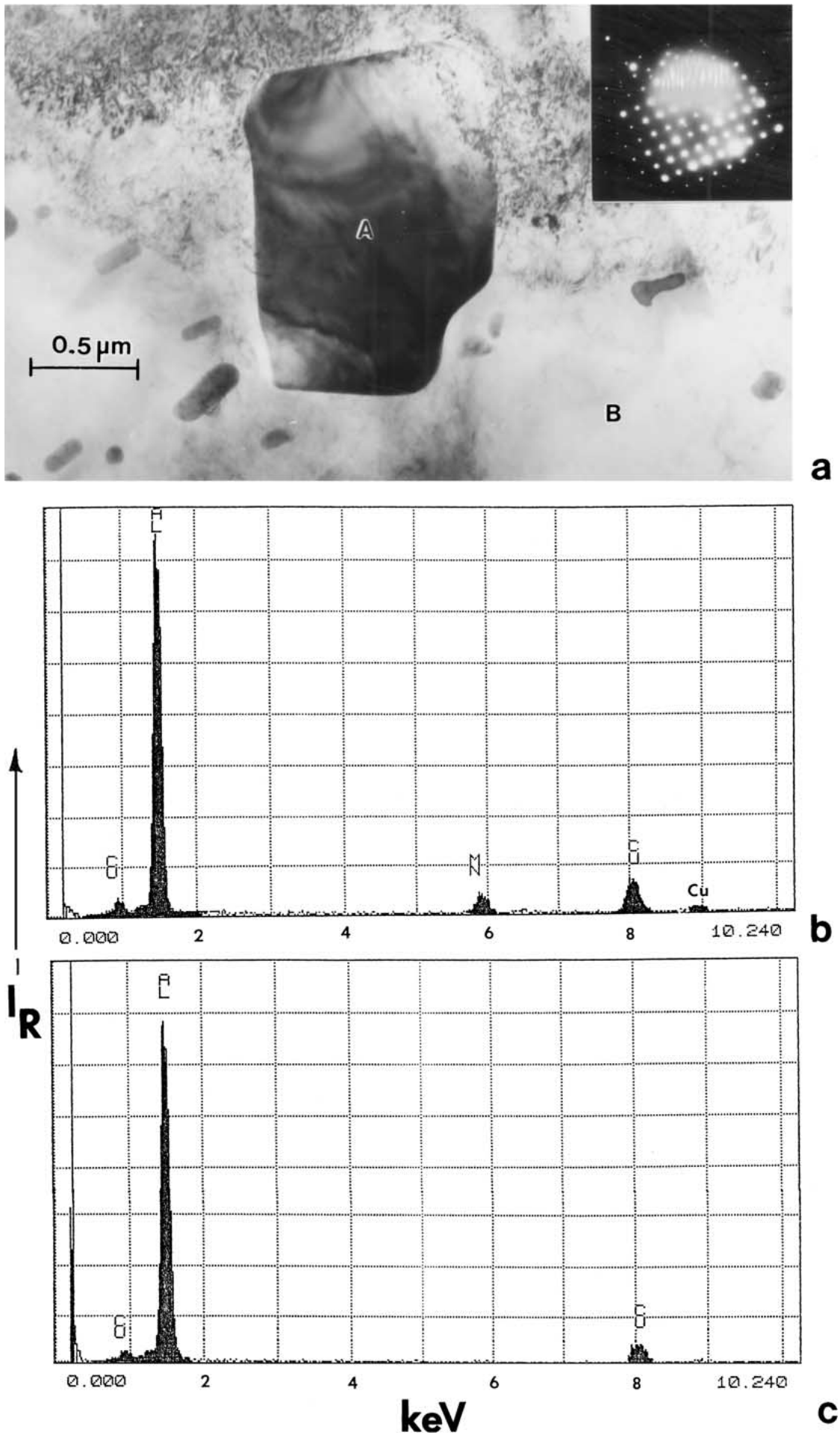

Figure 2 Example of large Al-Cu-Mn second-phase particle in aluminum alloy 2524. (a) TEM bright-field image with SAED pattern insert for particle region marked A. (b) EDX spectrum for particle A in (a). (c) EDX reference spectrum for alloy matrix region marked B in (a).

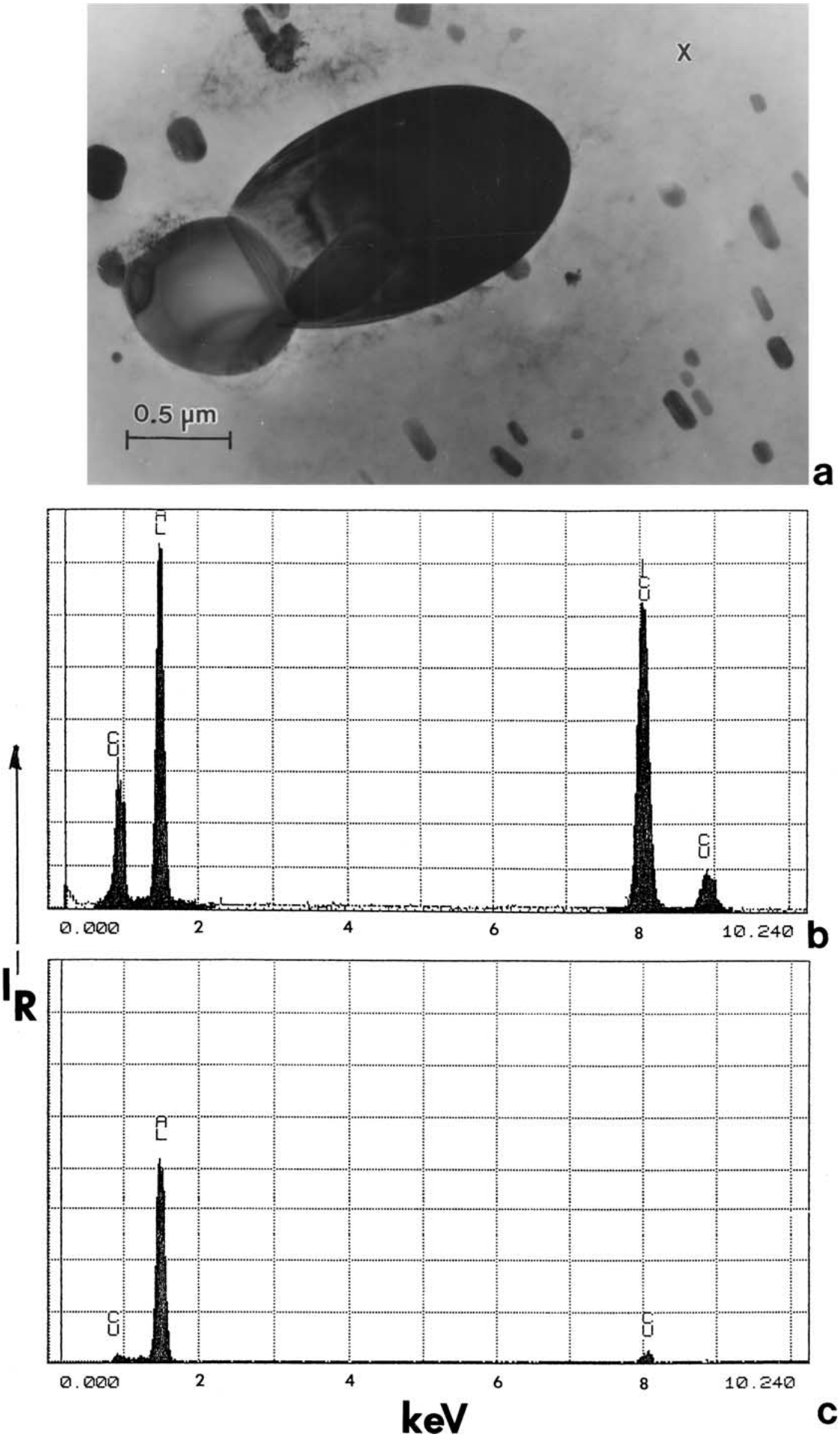

Figure 3 Example of large Al-Cu second-phase particles in aluminum alloy 2524. (a) TEM bright-field image. (b) EDX spectrum for the large particle in (a). (c) EDX reference spectrum at X in (a). Note small precipitate background is the same as shown in Figs 1 and 2.

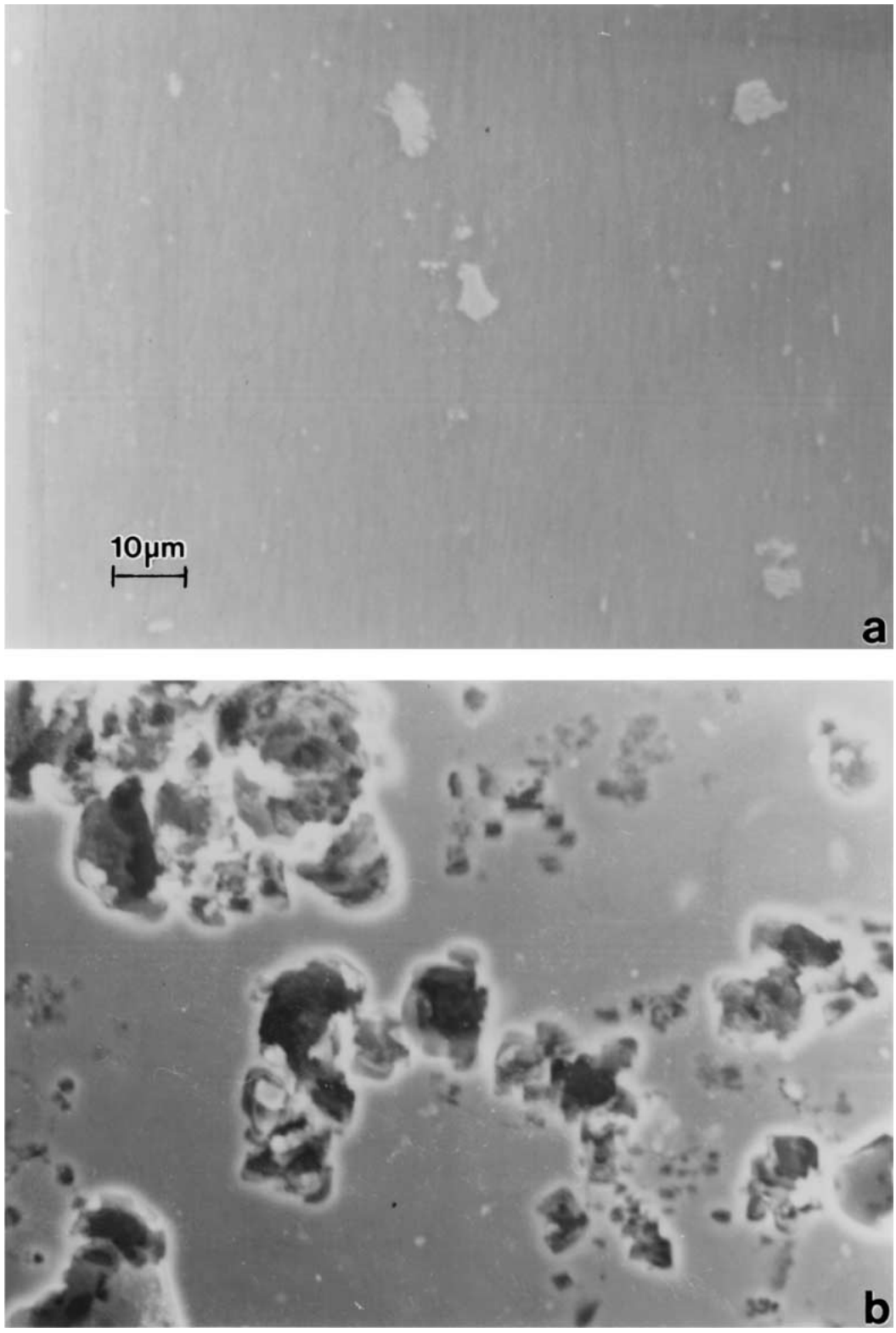

Figure 4 SEM views showing the starting test coupon surface prior to exposure to the NaCl solution environment (a), and a corroded surface for an aluminum alloy 2524 coupon tested (potentiostatically) in neutral NaCl solution for 3 minutes (b).

(0.6 M) NaCl solutions for 5 days (120 h). As in the previous work of Obispo *et al*. [1], three solution categories were utilized as comparative test environments: 1) an original or "neutral" 0.6 M NaCl solution with a nominal pH of 6; 2) an acidic 0.6 M NaCl solution adjusted to pH 3 using HCl; and 3) a basic 0.6 M NaCl solution adjusted to a pH of 11 using NaOH. The tests were conducted at a uniform temperature of ∼22°C. After immersion in these three solution regimes, which were not stirred, the coupons were rinsed in distilled water and ethanol. As in the original procedures developed by Obispo *et al*. [1], the solutions were not stirred in order to keep any remnant copper particles or clusters from redistributing over the surfaces.

Potentiostatic tests were also performed on the neutral NaCl solutions at −180 mV (corresponding to

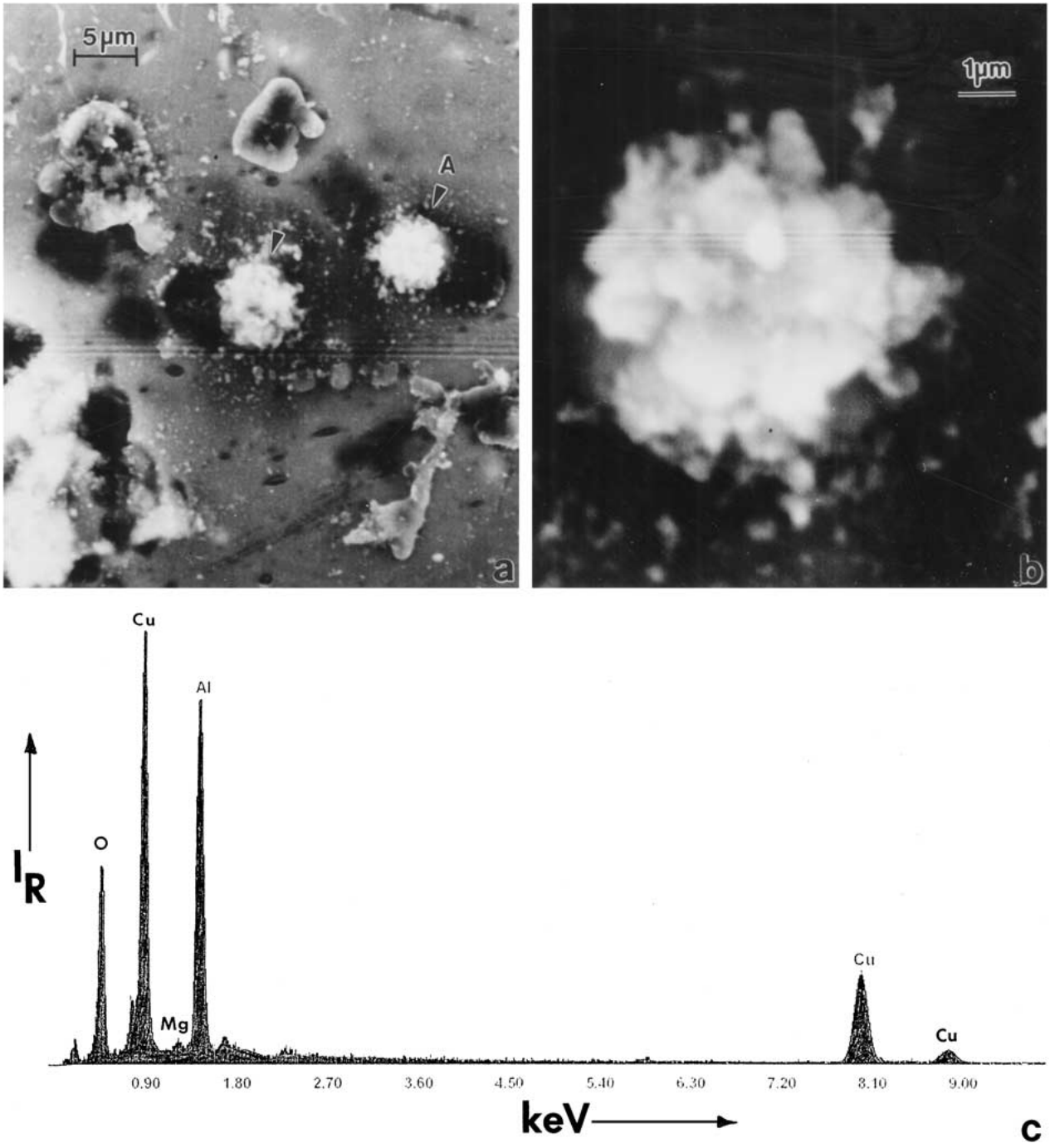

Figure 5 SEM views ((a) and (b)) and EDX spectrum (c) for copper particle clusters (arrows in (a)) observed on aluminum alloy 2524 after exposure to neutral (pH 6) NaCl solution as in Fig. 4. (b) Shows a magnified view of the lower Cu cluster in (a) (arrow A). (c) EDX spectrum for cluster in (b).

a current density of about 300 A/m^2) versus SCE; for a period of 3 minutes at 22°C. This value is slightly below the −200 mV utilized previously for Al 2024 [1].

Test coupons from the various corrosion regimes were initially examined by SEM and EDX after very light coating with sputtered Au to eliminate surface changing at a variety of reaction products and fine Cu clusters.

The replica-based, lift-off technique utilized by Obispo *et al*. [1] and described in some detail by them was employed to extract surface reaction products from the corresponding test coupons utilizing standard, 3 mm screen grids which could be examined in the TEM. In this extraction process, heavier Au sputtered films provided the extraction matrix. A Hitachi H-8000 analytical TEM fitted with a goniometer-tilt stage and a Noran EDX spectrometer system was utilized in observing the screen grids at an operating voltage of 200 kV.

In order to examine the intrinsic Al 2524 microstructure, especially the precipitates test coupons in their initial, untested state were ground to thicknesses of ∼0.2 mm and 3 mm discs punched from these thin sections for preparing TEM thin films. These punched discs were electropolished to provide electron transparent regions in a Tenupol-3, dual-jet electropolisher using a solution of 20% nitric acid in methanol at −30°C. These TEM thin sections were currently examined to develop

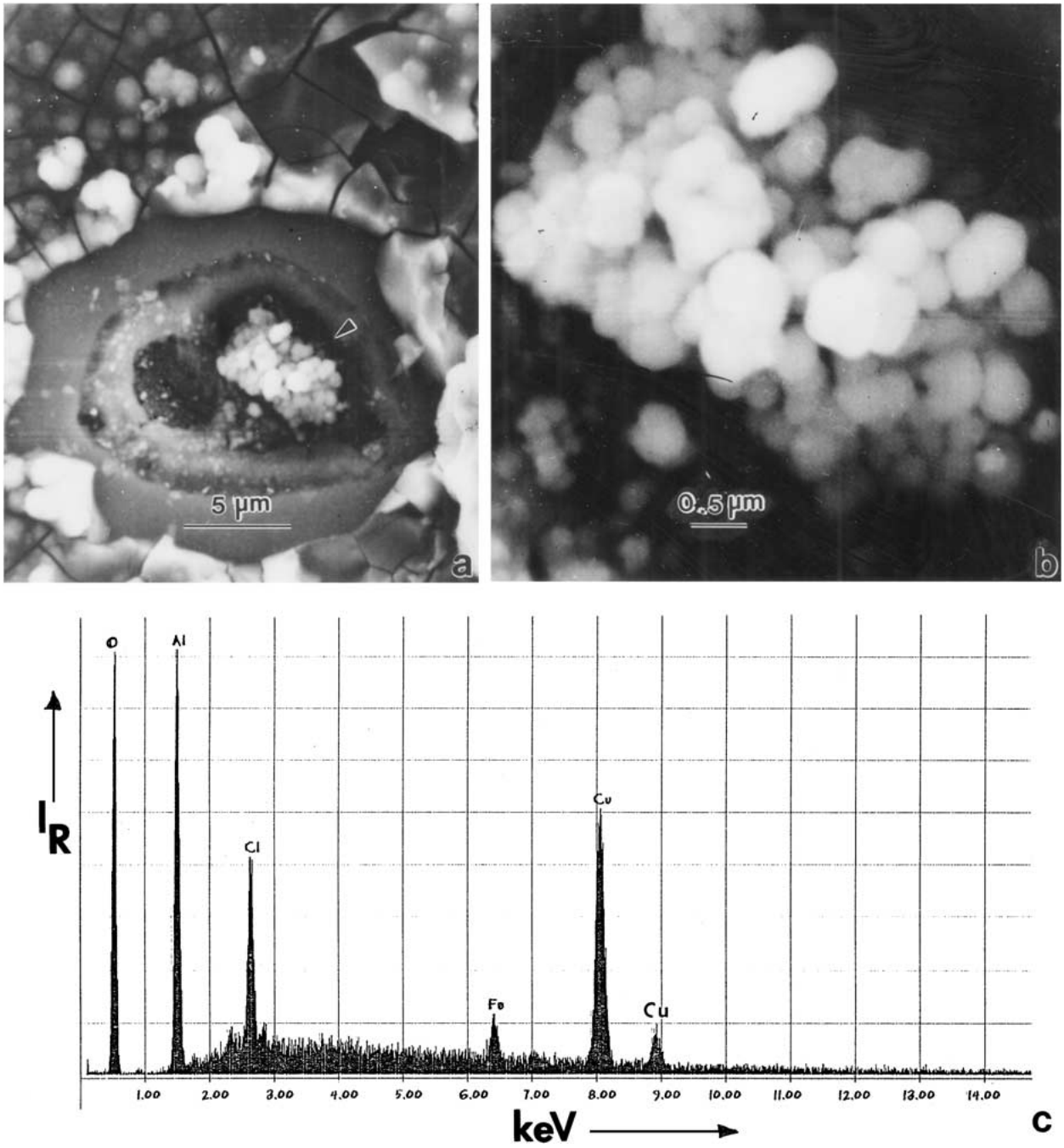

Figure 6 SEM views ((a) and (b)) and EDX spectrum (c) for copper particle cluster in a large corrosion pit in an aluminum alloy 2524 exposed 5 days to acidic (pH 3) NaCl solution. (b) is a magnified view of (a).

a precipitate and second-phase particle inventory for comparison with inventories already developed for Al 2024 alloy samples [1, 3].

3. Results and discussion

3.1. TEM inventory of second-phase particles

Figs 1–3 illustrate the range of precipitates and second-phase particles in the aluminum alloy 2524, with Fig. 1 representing the propensity of precipitates to be Al-Cu-Mn-Fe. Fig. 2 shows a large Al-Cu-Mn precipitate/inclusion while Fig. 3 shows a large Al-Cu second-phase bi-particle inclusion. In both Figs 2 and 3 the background precipitates are essentially the same as those shown in Fig. 1, and these precipitates represent the primary type of second-phase particles in this alloy. The large inclusions shown in Figs 2 and 3 are commensurate in size with the larger inclusions observed in the aluminum alloy 2024 by Obispo *et al.* [1], except the compositions were generally different, especially in stoichiometries. In contrast to five prominent second-phase, large particle regimes noted by Obispo *et al.* [1] in Al 2024 and four prominent regimes in Al 2024 noted in earlier work by Buchheit *et al.* [4], the Al-Cu-Mn-Fe precipitates are the only dominant inclusions, and these are relatively small in size (≤ 0.5 μm) (Figs 1–3). Fig. 3 represents the only Cu-rich, large inclusions observed but not in any

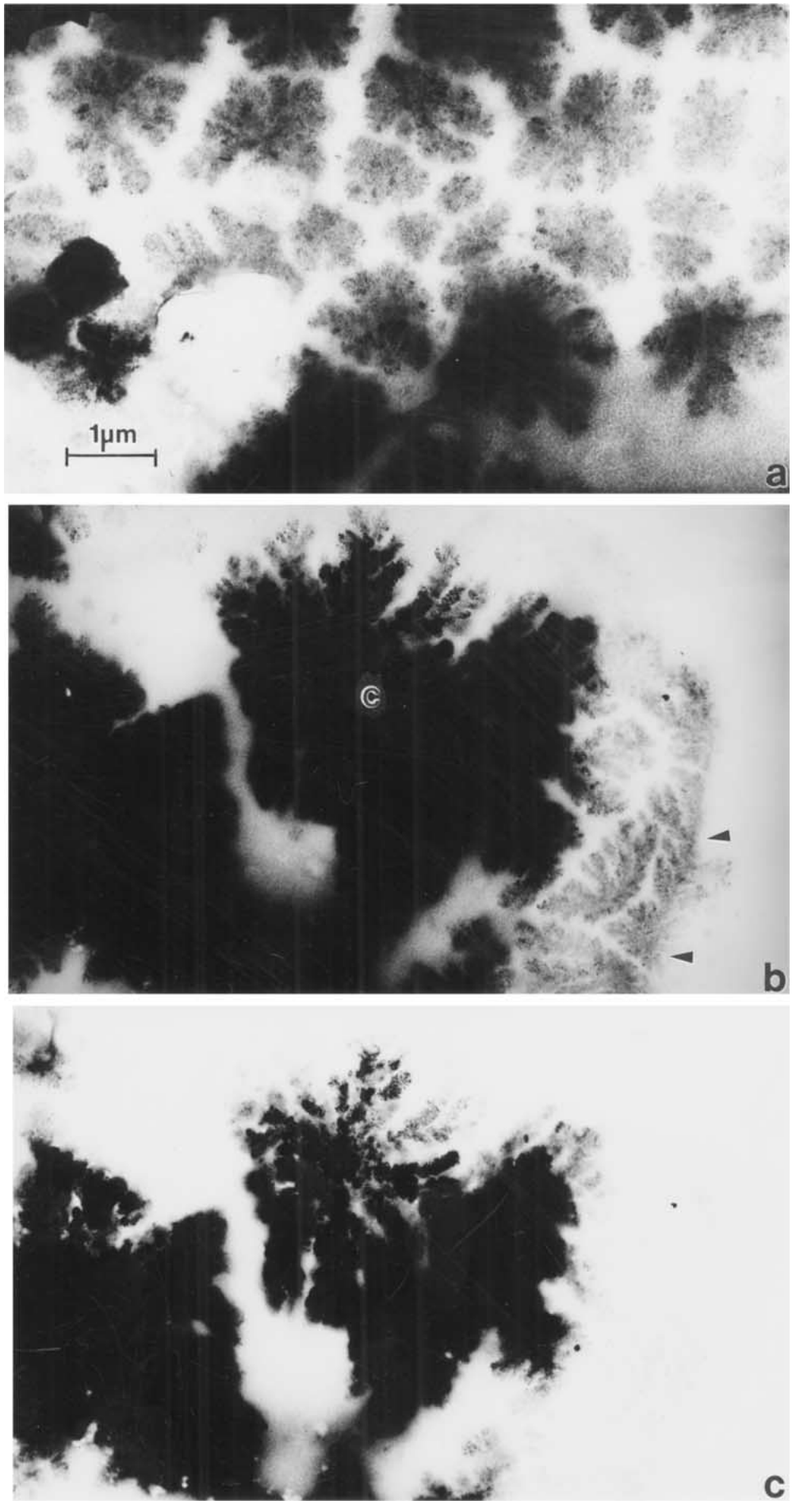

Figure 7 TEM bright-field images of copper deposit structure lifted (extracted) from the surface of aluminum alloy 2524 exposed to basic (pH 11) NaCl solution. (a) Numerous, microdendritic nuclei. (b) Nuclei (arrows) and larger microdendritic clusters. (c) Light exposure view showing microdendritic features in larger cluster marked C in (b).

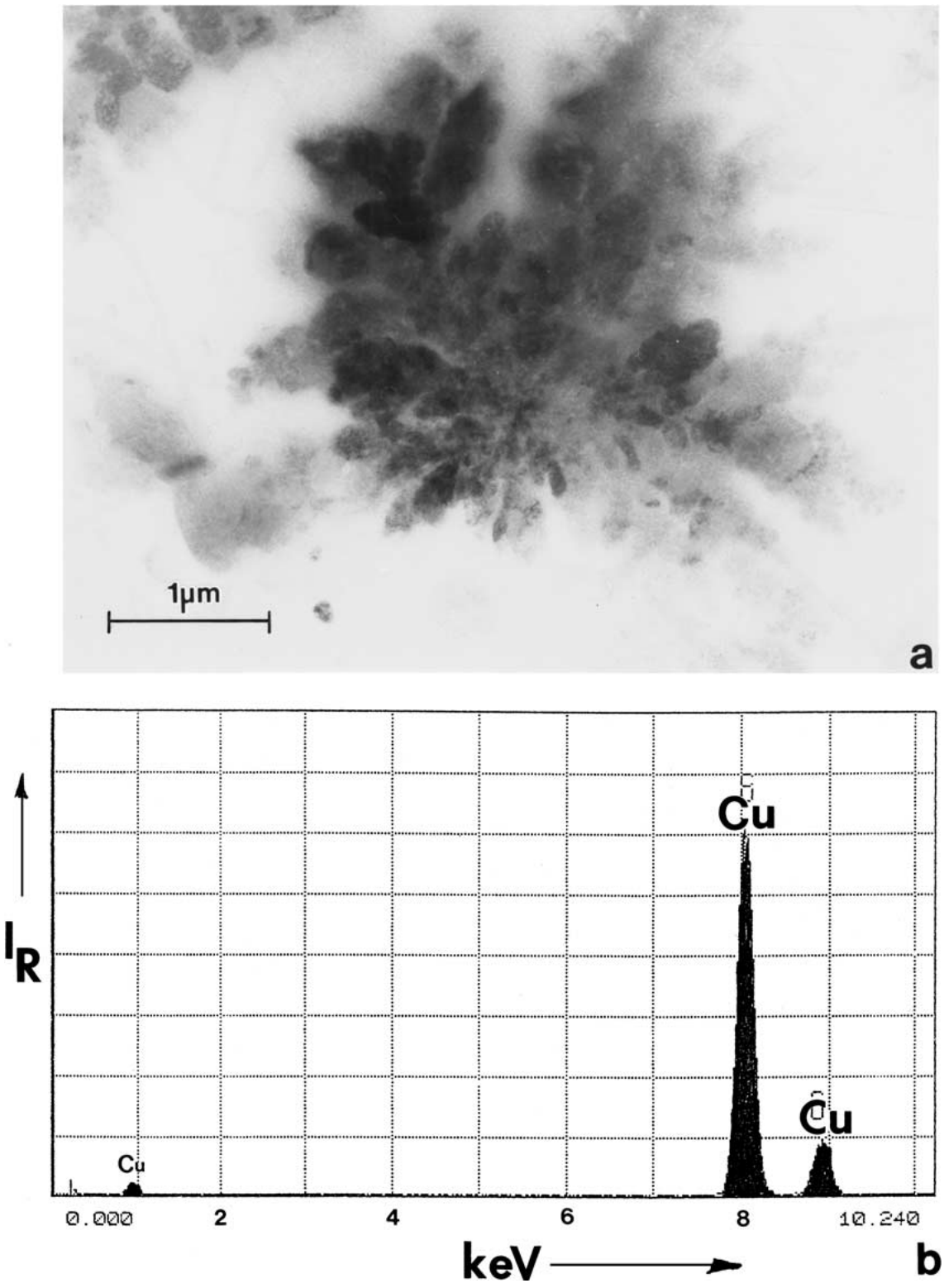

Figure 8 (a) Light exposure TEM image showing microdendritic Cu cluster in the same surface area illustrated in Fig. 7. (b) EDX spectrum for the Cu cluster in (a).

prominence in the microstructure. In contrast to the various Al 2024 regimes, the Al 2524 represents a relatively uniform second-phase regime with only a few large inclusions having significant Cu. There were no observations of large second-phase inclusions with significant Fe which were common in the Al 2024 samples of the previous work [3, 4]. Figs 1b and 2b illustrate that the Al-Cu-Mn-Fe and Al-Cu-Mn particles contain more copper than the matrix and as anodic or cathodic sites they could preferentially react to produce Cu^{2+} in solution.

3.2. SEM analysis of surface corrosion and surface-related products

Fig. 4 shows SEM views of the starting, polished coupon surface prior to any corrosion testing (Fig. 4a)

and the pitting observed after potentiostatic testing (at −180 mV) in a neutral (0.6 M) NaCl solution for 3 minutes (Fig. 4b). Fig. 5 shows a similar coupon surface section at a significantly higher magnification than Fig. 4b which shows loose, dendritic-like copper-rich clusters. In contrast to Fig. 5, Fig. 6 shows nodular-like, copper-rich clusters associated with a large pit surrounded by corrosion-related oxy-hydroxide deposits. Some residual Cl ion is also detected in the spectrum shown in Fig. 6c. Note the variance in cluster type (nodular versus micro-dendritic-like) on comparing Fig. 6b with Fig. 5b, respectively. Also note the considerably larger cluster in Fig. 6b for the acidic (pH 3) NaCl environment exposure for 5 days versus the neutral (pH 6) NaCl environment for only 3 minutes in Fig. 5b. Hydrolysis of the Al^{3+} ion can lead to pH changes during the corrosion process. In the present experiments, use of a pH meter before and after the corrosion test demonstrated that there was no significant pH change in the test cell.

3.3. TEM analysis of test coupon surface lift-off replicas

Figs 7 and 8 illustrate, in contrast to Figs 5 and 6, typical views of copper clusters growing on test coupon surfaces after 5 days exposure to basic (pH 11) NaCl immersion environments. These views, at much higher magnifications than those associated with the SEM images in Figs 5 and 6, show classical microdendritic structures even more pronounced than that shown in a neutral environment (∼pH 6) in Fig. 5b. Fig. 8b shows only copper in the corresponding EDX spectrum for the micro-dendritic cluster shown in Fig. 8a, and is typical of numerous, similar analyses performed on a wide range of surface-extracted clusters.

The images of copper clusters illustrated in Figs 5b, 6b and 8a correspond exactly to the cluster morphologies originally described by Obispo *et al.* [1] for aluminum alloy 2024 in the same pH environments. Consequently, it is reasonable to conclude that the mechanism of nucleation and growth of copper clusters on the two alloys are characteristically identical.

4. Summary and conclusions

Observations of the nucleation and growth of copper clusters on aluminum alloy 2524 (4.5% Cu) sheet specimen surfaces during corrosion have confirmed the original observations and conclusions involving Cu clusters depositing on Al 2024 (4% Cu) surfaces. In both studies, samples were exposed to identical test environments (0.6 M NaCl at three pH levels: 3, 6 and 11). The morphological features of the Cu clusters were identical to those previously observed by Obispo *et al.* [1]: dendritic in basic to neutral NaCl solutions (pH 11 to 6) and nodular/botryoidal in acidic NaCl solutions (∼pH 3). Unlike other NaCl corrosion studies involving Al 2024, there were no significant observations of large inclusions or large Cu or Fe-rich inclusions acting as preferred deposition sites for the Cu. These observations support the original electrochemical displacement reaction mechanism proposed by Obispo *et al.* [1] where Cu in Cl^- solutions is deposited onto a more electropositive, aluminum-rich substrate. In this reaction on copper-rich aluminum alloys (such as 2024 and 2524) Cu^{2+} is released into the solution by corrosion of the matrix. A previous paper describes an experiment which verified that enough copper is released by corrosion of alloy 2024 to raise the copper ion concentration in the whole test cell (about 500 ml) by a detectable amount [1]. In the absence of vigorous stirring, Cu^{2+} would be expected to concentrate in a solution layer at the metal surface. At the surface in contract with this enriched solution, Cu^{2+} is reduced. Free copper nucleates and grows as clusters, whose morphologies change with pH as noted. This Cu cluster growth causes additional pitting or promotes pitting around the nucleation/growth site, releasing Al^{3+} and some additional Cu^{2+}. These galvanically coupled electrochemical processes (anodic dissolution of Al and cathodic deposition of Cu) are like the electrochemical displacement reactions that occur during "cementation" of copper from minewaters onto iron or aluminum scrap.

Consequently, it now appears that any copper-containing aluminum alloy (with Cu in the range of 2 to 5 weight percent) will exhibit enhanced pitting corrosion because of the copper deposition on the aluminum alloy surface. Production of so-called "clean" alloys with reduced numbers of certain precipitates and inclusions may well improve fatigue resistance and other properties. However, this approach will likely not eliminate copper-cluster formation and its role in stimulating pitting corrosion over extended areas of the alloy surface.

Acknowledgments

This research was supported by the Air Force Office of Scientific Research (F49620-95-1-0518) through the FAST Center for Structural Integrity of Aerospace Systems at the University of Texas at El Paso. We are grateful for the help of Dr. Elizabeth Trillo in applying the lift-off technique for TEM analysis. We also appreciate the help of Lola Norton in assisting with corrosion product analysis in UTEP's environmental scanning electron microscope.

References

1. H. M. OBISPO, L. E. MURR, R. M. ARROWOOD and E. A. TRILLO, *J. Mater. Sci.* **35** (2000) 3479.
2. R. S. ALWITT, in "Oxides and Oxide Films," Vol. 4, edited by V. W. Diggle and A. K. Vijh (Marcel Dekker, Inc., New York, 1976) p. 3.
3. G. S. CHEN, M. GAO and R. P. WEI, *Corrosion Science* **52**(1) (1996) 8.
4. R. G. BUCHHEIT, R. P. GRANT, P. F. HLAUA, B. McKENZIE and G. L. BENDER, *J. Electrochem. Soc.* **144**(8) (1997) 2621.

Received 18 October 2000
and accepted 24 April 2001